Desalination and Water Treatment
www.deswater.com
doi: 10.1080/19443994.2013.807477

52 (2014) 5401–5412
August

Taylor & Francis
Taylor & Francis Group

Preparation and characterization of charcoal from feathers and its application in trimethoprim adsorption

Cheng Cheng, Jian Zhang*, Chenglu Zhang, Hai Liu, Weifeng Liu

Shandong Key Laboratory of Water Pollution Control and Resource Reuse, School of Environmental Science and Engineering, Shandong University, Jinan 250100, China
Tel. +86 531 88363015; Fax: +86 531 88364513; email: zhangjian00@sdu.edu.cn

Received 8 March 2013; Accepted 11 May 2013

ABSTRACT

Feathers were utilized to prepare charcoal which could be used for the adsorption of the antibiotic trimethoprim (TMP). The physicochemical properties of the feather-derived charcoal were determined. The feather-derived charcoal had a surface area of 805.4 m^2/g and a well-developed microporous structure. The contents of acidic and basic functional groups on feather-derived charcoal were 1.36 and 1.76 mmol/g, respectively, and $pH_{pzc} = 7.52$. We studied the influences of adsorbent dose, initial TMP concentration, agitation time, temperature, pH, and ionic strength on the adsorption. The desorption properties of TMP-sorbed feather-derived charcoal were also tested. The adsorption kinetics accorded with the pseudo-second-order kinetic equation, and the overall rate of adsorption was mainly controlled by intra-particle diffusion. The adsorption isotherms for the TMP-feather-derived charcoal system are explained better by the Freundlich isotherm at lower temperature (293 K) while the Langmuir isotherm gave a better fit at higher temperature (313 K). It is considered that a combination of hydrophobic interactions and ion exchange as well as electrostatic interaction was the adsorption mechanisms.

Keywords: Feather-derived charcoal; Trimethoprim; Adsorption; Mechanism; Desorption

1. Introduction

Huge amounts of feathers, especially chicken feathers, are discarded during poultry processing. This causes that over hundreds of millions tons of chicken feathers are generated in the world every year. They are treated as a waste product and only a small portion is utilized because the procedures for the utilization of feathers are difficult [1]. Feathers are mainly composed of keratin, a hard to degrade and insoluble animal protein [2]. In most cases, the feathers are disposed of by burial [3]. But, many examples are available in the literature concerning the use of feathers as adsorbents, for example, hen feathers were used as an adsorbent to remove dye from aqueous solutions [4–6], raw chicken feathers were utilized for the uptake of heavy metals [7–9], and chicken feathers were used for the removal of phenol from aqueous solutions [10]. However, no studies have been published on preparing feather-derived charcoal for use as an adsorbent. Adsorption is widely used in the removal of contaminants from wastewater [11–18]. Considering the economic benefit, chicken feathers were taken as a potentially suitable

---

*Corresponding author.

precursor to prepare adsorbents because they are available in significant amounts.

Trimethoprim (TMP) is among the most important synthetic antibiotics used in human and veterinary medicine worldwide. Antibiotics are widely used as medicines and animal growth promoters, and these chemicals are now receiving more attention as water-borne pollutants. Unlike many other aquatic pollutants, antibiotics act directly on microbes and can contribute to the development of antibiotic resistance [19]. In many cases, these drugs are emitted continuously to the environment from farming or ranching business, thereby acting as persistent pollutants despite their rapid degradation [20]. It is impossible to halt the use of antimicrobial agents, so management of their disposal is an important strategy to control their contamination of water resources [21].

In this work, a low-cost adsorbent prepared from chicken feathers, feather-derived charcoal, was developed and used to remove the antibiotic TMP from aqueous solutions. The objectives of this study were (1) to prepare and characterize the physical and chemical properties of feather-derived charcoal; (2) to evaluate the adsorption behavior of feather-derived charcoal toward TMP by investigating the effect of adsorbent dose and initial TMP concentration, as well as studying the adsorption kinetics, isotherms, and thermodynamics; (3) to determine the mechanisms of interaction between feather-derived charcoal and TMP by analyzing the effect of pH, temperature, and ionic strength, as well as the desorption characteristics of feather-derived charcoal and TMP.

2. Materials and methods

2.1. Materials

All solutions were prepared with distilled water. All of the reagents were of analytical reagent grade. TMP (Ultra pure grade) was purchased from Aladdin Chemistry Co. (Shanghai, China) and used as received.

The chemical structure and basic properties of TMP, 2,4-diamino-5-(3,4,5-trimethoxybenzyl)-pyrimidine are shown in Table 1.

2.2. Preparation of feather-derived charcoal

Chicken feathers obtained from a farmers' market were washed with distilled water to remove impurities. After drying at 80 °C for 24 h, they were crushed using a high-speed pulverizer into small particles which had a fluffy appearance. Afterward, the crushed feathers were immersed in 45 wt.% phosphoric acid solution with H_3PO_4:chicken feather ratio of 2:1(w:w). The mixture was steamed at 105 °C for 20 min under high pressure (0.15 MPa) and then heated in a tube furnace (SRJK-2–13, Beijing) up to 600 °C and kept for 50 min. After carbonization and activation, the sample was allowed to cool down to ambient temperature naturally. The obtained product was washed using distilled water repeatedly until the pH remained close to neutral, then dried at 105 °C for 12 h. Finally, it was sieved to 100–160 mesh with standard sieves.

2.3. Characterization of sorbent

A scanning electron microscope (S4800, Hitachi, Japan) was used to visualize the surface morphology and structure of chicken feathers and feather-derived charcoal.

The surface area and porous properties of the feather-derived charcoal were determined using a surface-area analyzer (QuantaChrome Corporation, USA) based on the N_2 adsorption at 77 K. The Langmuir surface area (S_L) and the Brunauer–Emmett–Teller surface area (S_{BET}) were calculated by the manufacturer's software. Pore structure information was estimated following the Density Functional Theory method. The micropore surface area (S_{mic}), external surface areas (S_{ext}) and the micropore volume (V_{mic}) as well as the total pore volume (V_{tot}) were calculated

Table 1
Basic information of trimethoprim

	Molecular weight	Chemical structure	Melting point (°C)	pK_a
TMP	290.32	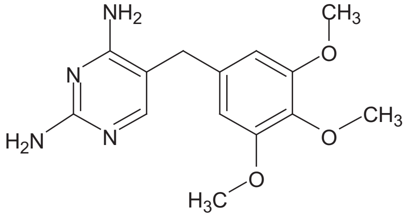	199∼203	7.30

by the t-plot method. The mean pore diameter D_p was calculated as $D_p = 4V_\mathrm{tot}/S_\mathrm{BET}$.

The content of C, H, N, O, and S of chicken feathers and feather-derived charcoal was measured using a Vario EI III Element Analyzer (USA). The functional groups available on the surface of feather-derived charcoal were recorded using a Fourier transform infrared (FT-IR) spectrometer (Fourier-380 FT-IR, America) in the spectral range 4,000–400 cm^{-1}.

The point of zero charge ($\mathrm{pH_{PZC}}$) of feather-derived charcoal was determined by means of the following procedure [22]. The concentrations of various acidic and basic functional groups on the feather-derived charcoal's surface were determined by the Boehm titration method [23] with the assumption that $NaHCO_3$-neutralized carboxyl groups; Na_2CO_3-neutralized carboxyl and lactone groups; NaOH neutralized carboxyl, lactone, and phenolic groups; and HCl-neutralized basic groups.

2.3. Batch equilibrium studies

Batch equilibrium experiments were performed to investigate the effects of adsorbent dose, initial concentration, agitation time, temperature, solution pH, and ionic strength on the adsorption. A set of 150-mL stoppered conical flasks containing 50-mL TMP solution and 0.0100 ± 0.0002 g feather-derived charcoal were agitated at 120 rpm in an isothermal water bath shaker for 60 h to ensure that they reached equilibrium. Then, the adsorbents were filtered using syringe filter through 0.45-μm membrane filters and the residual TMP concentrations were determined with a UV–visible spectrophotometer (UV-754, Shanghai) from the absorption at the maximum absorption wavelength of 275 nm.

The ionic strengths of the experimental solutions were adjusted using NaCl solutions. The initial solution pH was adjusted to 2–12 by adding different concentrations (0.01 and 0.1 M) of HCl or NaOH solutions. The pH values were measured with a pH meter (Model pHS-3C).

To examine the effect of temperature on the adsorption, adsorption isotherms at three different temperatures (293, 303 and 313 K) were studied without adjusting solution pH.

2.4. Batch kinetic studies

Adsorption kinetic experiments were conducted to investigate the effect of agitation time on the sorption and determine the kinetic parameters. The experiments were carried out using three 1 L capacity glass breakers. For these tests, 0.2 g feather-derived charcoal was added into 1,000 mL TMP solutions with different ionic strengths and the mixture was stirred on an electromagnetic stirrer (Model 78–1) at 20 ± 1 °C and 400 rpm. The aqueous samples were withdrawn and filtered at predetermined time intervals (0–60 h) and analyzed to determine the equilibrium concentrations of TMP solution using the same method as described above.

2.5. Desorption experiments

After the equilibrium sorption experiments, the adsorbent was filtered and washed repeatedly with distilled water to remove any unadsorbed TMP molecules. After drying at 40 °C for 12 h, desorption treatments were tested by adding 50 mL of either (1) distilled water, (2) 0.1 M NaCl, (3) 1 M NaCl, (4) 0.1 M HCl, or (5) 90% ethyl alcohol to the solid.

3. Results and discussion

3.1. Characteristics of adsorbent

3.1.1. Physical properties of the absorbent

Scanning electron microphotograph (SEM) images of chicken feathers and feather-derived charcoal are shown in Fig. 1. Compared to the original chicken feathers, the feather-derived charcoal had a coarser surface with irregular pores, confirming the powerful effect of phosphoric acid. Fig. 1(c) illustrates the N_2 adsorption/desorption isotherms of the feather-derived charcoal sample. According to the classification of adsorption isotherm types by the International Union of Pure and Applied Chemistry (IUPAC) [24], the adsorption isotherm belongs to type I, in which the adsorption quantity increases rapidly as the pressure increases and finally reaches a limiting value. Additionally, the pore size distribution curve calculated from the adsorption isotherm can be applied to analyze the porosity of the feather-derived charcoal. As shown in Fig. 1(c), the pores of the feather-derived charcoal are mostly located in the range of 0–2 nm with an average pore width of 1.759 nm, indicating a microporous structure of the adsorbent. The surface area of the sample was calculated using the Langmuir method ($S_L = 805.4\,\mathrm{m^2/g}$) and the Brunauer–Emmett–Teller method ($S_\mathrm{BET} = 589.0\,\mathrm{m^2/g}$), with a total pore volume of $0.259\,\mathrm{cm^3/g}$. The pore structure parameters and the yield of the charcoal are listed in Table 2. The data demonstrate that the contribution of micropores to the total pore volume is above one-half; therefore, the feather-derived charcoal was micro-porous with a relatively large surface area.

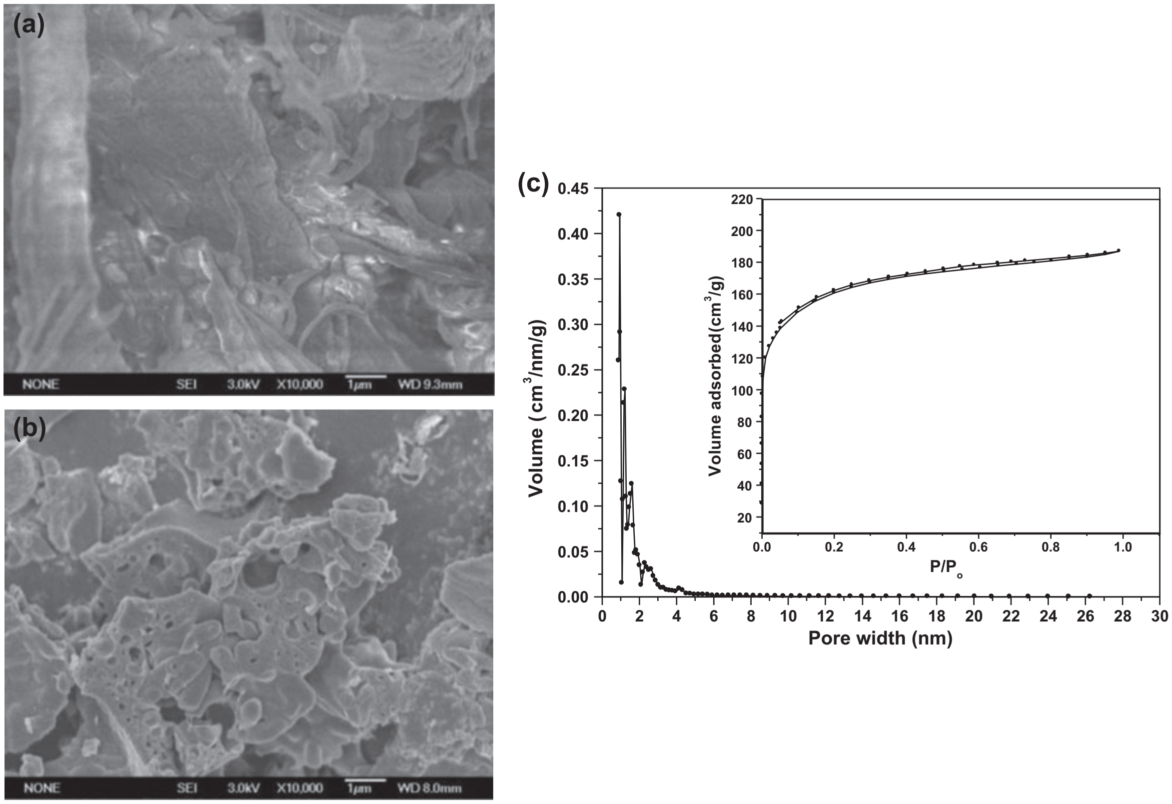

Fig. 1. SEM of chicken feathers (a) and feather-derived charcoal (b) at 10,000; pore size distribution of feather-derived charcoal (c). Inset shows its N_2 adsorption/desorption isotherms.

Table 2
Pore structure parameters and the yield of feather-derived charcoal

S_L (m^2/g)	S_{BET} (m^2/g)	S_{mic} (m^2/g)	S_{ext} (m^2/g)	V_{tot} (cm^3/g)	V_{mic} (cm^3/g)	V_{mic}/V_{tot} (%)	Dp (nm)	Yield (%)
804.4	589.0	483.8	105.2	0.259	0.205	79.15	1.759	28.7

Table 3
Chemical composition of chicken feathers and feather-derived charcoal (wt.%, maf[a])

	C	O	N	H	S
Chicken feather	48.21	27.23	14.20	7.98	2.39
Feather-derived charcoal	47.28	43.13	6.87	2.30	0.41

[a] maf—moisture and ash free.

3.1.2. Chemical properties of the adsorbent

The chemical compositions of chicken feathers and feather-derived charcoal obtained in this work are shown in Table 3. The feather-derived charcoal has an almost equal content of carbon and a much higher content of oxygen while a lower content of hydrogen and nitrogen compared to chicken feathers. The chemical changes that occurred in the chemical activation and carbonization process facilitated the removal of hydrogen and nitrogen, and resulted in an increased oxygen content [25]. It is probable that oxygen in the air combined with hydrogen and nitrogen and was released as H_2O, NO, or NO_2 and some oxygen combined with the carbon and was trapped in the charcoal.

The identity and quantity of functional groups on the charcoal surface play an important role in most of the applications of carbon materials. These

Table 4
Concentration of surface functional groups on feather-derived charcoal

Feather charcoal	pH_{pzc}	Carboxyl (mmol/g)	Lactones (mmol/g)	Phenol hydroxyl (mmol/g)	Total acidic (mmol/g)	Total basic (mmol/g)	Total groups (mmol/g)
	7.52	0.228	0.635	0.496	1.36	1.76	3.12

functionalities have been traditionally separated into two families: (1) carboxyl groups, anhydrides, lactones, phenol, and lactol groups account for the acidic character, (2) cyclic ketones and pyrone-like groups are the likely basic oxygen-containing functional groups [26]. Table 4 lists the contents of the surface functional groups and the pH_{pzc} of our feather-derived charcoal. The nearly neutral pH_{pzc} is probably caused by the relatively large amounts of both weakly acidic and weakly basic functional groups on its surface.

FT-IR analysis permits spectrophotometric observation of the adsorbent surface in the range 4,000–400 cm^{-1} and serves as a direct means for the identification of the organic functional groups on the charcoal's surface. The infrared spectra of feather-derived charcoal and feather-derived charcoal with adsorbed TMP are shown in Fig. 2. For the as-prepared charcoal, the peak occurring at 1,540 cm^{-1} is characteristic of carboxylic and amino groups [27]. C–O–H deformation with simultaneous carbon ring vibrations results in a strong IR absorption in the 1,420–1,480 cm^{-1} region [26]. The band at 1,460 cm^{-1} is typical of oxidized carbons attributed to O–H deformation in carboxyl groups; therefore, the bands at around 1,461 cm^{-1} are suggested to be from carbonylic groups. The peaks at about 1,177 and 1,034 cm^{-1} represented C–O vibrations of various oxygen-containing groups [28,29]. The FT-IR spectra in the 668–750 cm^{-1} region show absorption bands due to aromatic structures. Above all, the feather-derived charcoal adsorbent mainly contained carbonyl groups and aromatic structures after activation.

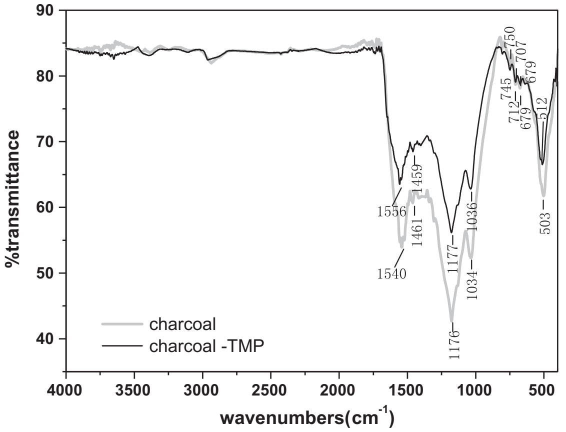

Fig. 2. FT-IR spectra of feather-derived charcoal and feather-derived charcoal-TMP.

3.2. Adsorption mechanism

3.2.1. Effect of ionic strength

Fig. 3(a) shows the effect of ionic strength on the adsorption of TMP. The adsorption capacity decreased slightly with the increasing ionic strength, indicating that the adsorption of TMP mainly proceeds through inner-sphere complexes. Combined with the FT-IR results in Fig. 2, feather-derived charcoal-TMP showed

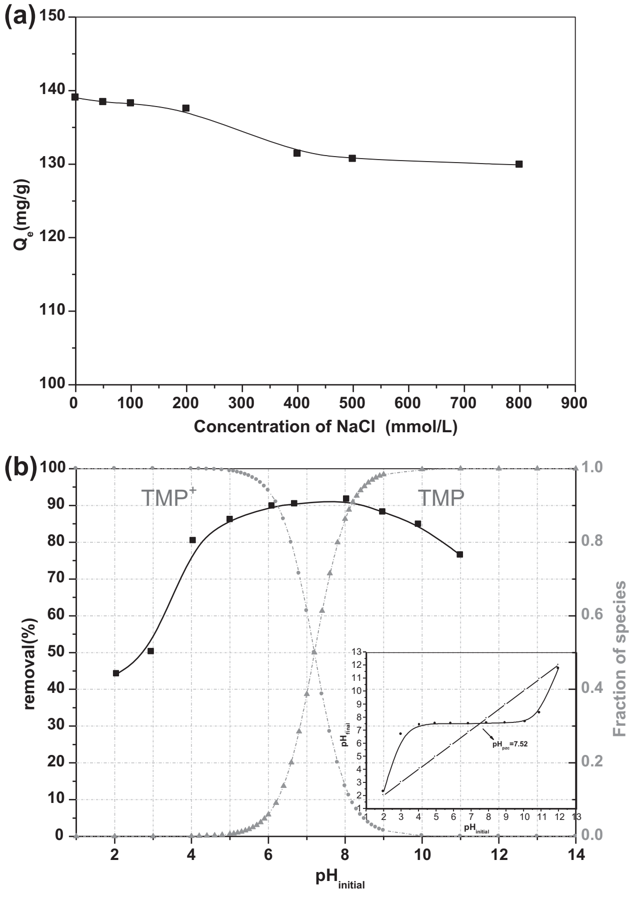

Fig. 3. Effect of ionic strength (a) and initial pH (b) on the adsorption of TMP and pH_{pzc} of feather-derived charcoal (inset b). (agitation time = 60 h, $C_0 = 0.1$ mmol/L, sorbent dose = 0.2 g/L, $T = 298$ K).

similar characteristic bands as feather-derived charcoal, except for a slight shift from 1,540 to 1,556 cm^{-1}, which could be due to physical interaction between the charcoal and the TMP adsorbate.

3.2.2. Effect of solution pH on adsorption

The pH of the antibiotic solution influences not only the surface charge of the adsorbent, but also the degree of ionization of TMP and the dissociation of functional groups on the active sites of the adsorbent [30]. The effect of pH on the adsorption of TMP on feather-derived charcoal was studied at 298 K. The removal percentage of TMP on feather-derived charcoal at different pH values is plotted in Fig. 3(b). It is obvious that the removal efficiency increased greatly between pH 2 and 4, gently increased between pH 4 and 7, and decreased from pH 8 to 11. The maximum equilibrium adsorption amount of 139.54 mg/g was achieved at about pH 7.5, close to the p*K*a value of TMP.

The influence of pH on the adsorption was not obvious under weakly acidic or weakly basic pH conditions (pH 6–9). Therefore, the adsorption of TMP is influenced more by the surface charge of feather-derived charcoal than by the solution pH. As discussed above, TMP was combined with the feather-derived charcoal by physical interaction. Another important mechanism controlling the adsorption of TMP might be Lewis acid–base interactions, wherein $–NH_2$ serves as the Lewis base and the O-containing groups on carbon serve as Lewis acids. At high pH, some of the Lewis acid sites were ionized and the Lewis acid–base interaction was weaker; therefore, the adsorption onto feather-derived charcoal decreased.

At low pH conditions, all of the TMP (T:) is in protonated form [31,32]:

$$TH^+ \leftrightarrow T: + H^+ \quad (1)$$

The protonated form of TMP was strongly adsorbed to the negatively charged sites of feather-derived charcoal surface by ion-exchange process and electrostatic attraction, which enhanced the amount adsorbed. However, these two interactions were not the primary mechanisms. As the pH of the system decreased, the increasing H^+ concentration did not favor the adsorption. This is due to fact that a competition occurs between H^+ and protonated form of TMP molecules [33]. As a result of this competition, the amount of TMP adsorbed at low pH is very low.

3.3. Desorption studies

Desorption studies help to obtain further insight into the adsorption mechanism and to evaluate the feasibility of regenerating the spent adsorbent. The results of the desorption experiments are depicted in Table 5. There was little desorption (4.13%) with distilled water. NaCl solutions were employed to reflect the importance of electrostatic interaction. Less than 20% of the sorbed trimethoprim was recovered by desorption with NaCl solutions of various strengths, implying that electrostatic interactions did occur in the sorption process but this was not a major mechanism. As much as 49.13% of the sorbed trimethoprim was desorbed by the HCl solution. This result implied that strong chemical interactions should be the dominant mechanism in the sorption, which may originate from ion exchange. Ethyl alcohol was used to determine the role of hydrophobicity in TMP sorption. More than 64% of sorbed TMP was recovered by 90% ethyl alcohol, indicating a significant contribution of hydrophobic interaction to the adsorption.

3.4. Effect of agitation time and adsorption kinetics

Fig. 4(a) shows the effect of agitation time on the adsorption of TMP onto feather-derived charcoal at different ionic strengths (c_{NaCl} = 10 mmol/L, 100 mmol/L, 500 mmol/L). Similar trends were observed at all three ionic strengths: a very rapid initial adsorption over a few hours, followed by a longer period of much slower uptake. The equilibrium time was established up to 60 h, and the amounts of adsorption equilibrium are 139.18, 139.02, and 137.37 mg/g.

In order to identify the potential rate-controlling steps involved in the adsorption, three kinetic models—pseudo-first-order, pseudo-second-order, and intraparticle diffusion models—were applied to the experimental data to analyze the adsorption kinetics of TMP.

Table 5
Percentage of sorbed trimethoprim mass desorbed by various treatments

	Distilled water	0.1 M NaCl	1 M NaCl	0.1 M HCl	90% C_2H_5OH
Efficiency	4.14%	12.59%	19.18%	49.13%	64.64%

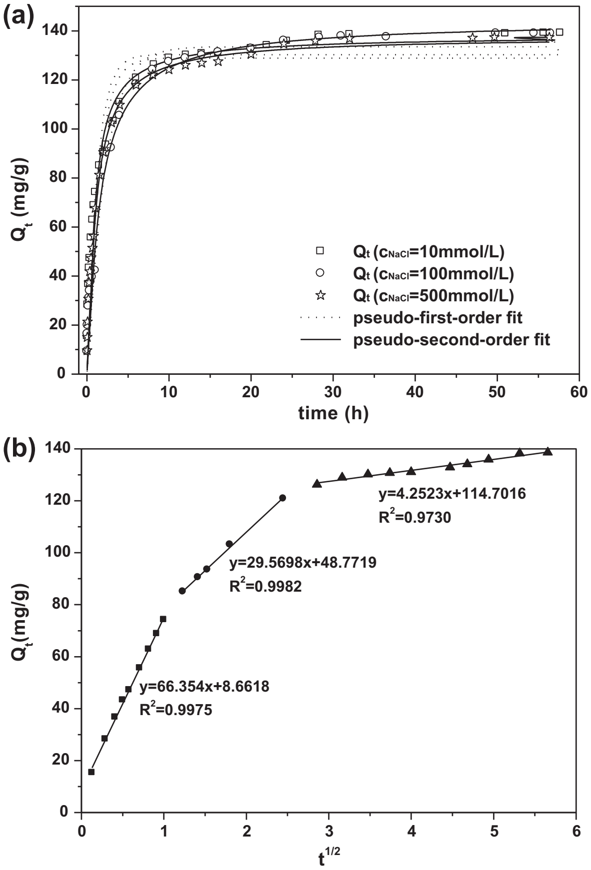

Fig. 4. Adsorption kinetics of TMP onto feather-derived charcoal fitted by pseudo-first-order (dots) and pseudo-second-order models (solid lines) (a), Intra-particle diffusion plots for adsorption of TMP onto feather-derived charcoal($c_{NaCl} = 10$ mmol/L) (b). ($C_0 = 0.1$ mmol/L, sorbent dose = 0.2 g/L, $T = 298$ K).

The pseudo-first-order equation can be expressed as [34]:

$$Q_t = Q_e(1 - e^{-k_1 t}) \tag{2}$$

where Q_e and Q_t are the amounts of TMP adsorbed at equilibrium and at time t (mg/g), respectively; and k_1 is the rate constant of the pseudo-first-order model (h^{-1}).

The pseudo-second-order kinetic model can be represented in the following form [35]:

$$Q_t = \frac{k_2 Q_e^2 t}{1 + k_2 Q_e t} \tag{3}$$

where k_2 is the rate constant of the pseudo-second-order adsorption (g/mg h).

The k_1, k_2, correlation coefficient, and Q_e (experimental and calculated) are summarized in Table 6. The correlation coefficients for the pseudo-first-order model were in the range of 0.9212–0.9710, and the calculated $Q_{e(cal)}$ values were lower than the experimental $Q_{e(exp)}$. For the pseudo-second-order kinetic model, the profiles showed a better agreement between the experimental and the calculated Q_e values, and the obtained R^2 values were between 0.9760 and 0.9880, indicating the suitability of the pseudo-second-order kinetic model to describe the adsorption process of TMP onto feather-derived charcoal.

The initial rate of sorption was estimated from pseudo-second-order kinetic model from the below equation:

$$h_{0,2} = k_2 Q_e^2 \tag{4}$$

The results were presented in Table 6. The highest initial rate of sorption was obtained at lowest ionic strength ($c_{NaCl} = 10$ mmol/L) in the studied range.

The half-sorption time, $t_{1/2}$ known as the time required for the sorption to take up half as much feather charcoal as its equilibrium value. This time is often used as a measure of the adsorption rate [36].

$$t_{1/2} = \frac{1}{k_2 Q_e} \tag{5}$$

The half-sorption time values at different temperatures were presented in Table 6. The lowest half-sorp-

Table 6
Kinetic model parameters for TMP

	c_{NaCl}	$Q_{e(exp)}$	Pseudo-first-order kinetic model			Pseudo-second-order kinetic model				
	(mmol L^{-1})	(mg g^{-1})	k_1 (h^{-1})	$Q_{e(cal)}$ (mg g^{-1})	R^2	$k_2 \times 10^{-3}$ (g (mg h)$^{-1}$)	$Q_{e(cal)}$ (mg g^{-1})	$h_{0,2}$ (mg $g^{-1}h^{-1}$)	$t_{1/2}$ (h)	R^2
Feather charcoal	10	139.18	0.82	130.29	0.9212	3.29	138.16	62.81	2.20	0.9760
	100	139.02	0.46	133.50	0.9711	3.28	144.26	68.20	2.12	0.9831
	500	137.37	0.73	128.90	0.9610	2.76	137.76	52.44	2.63	0.9880

tion time was obtained at lowest ionic strength ($c_{NaCl} = 10\,mmol/L$) in this study.

Distinguishing between the pseudo-first-order and pseudo-second-order kinetic models is not sufficient to identify the diffusion mechanism. The intraparticle diffusion model was used to predict the rate-controlling step. The equation for the model can be expressed as [37]:

$$Q_t = k_{int}t^{1/2} + C \tag{6}$$

where k_{int} is the intraparticle diffusion rate constant ($mg/g\,h^{1/2}$) and C is the intercept, which represents the thickness of the boundary layer. A larger intercept means a greater effect of the boundary layer [38].

It is generally accepted that the adsorption process consists of three continuous steps [39]: transport of adsorbate molecules from the bulk solution to the adsorbent external surface through boundary layer diffusion; diffusion of the adsorbate from the external surface into the pores of the adsorbent; and adsorption of the adsorbate on the active sites on the internal surfaces of the pores. The plots of q_t against $t^{1/2}$ are shown in Fig. 4(b). The curve shows three linear portions, indicating the different stages in adsorption. The third step is much slower in comparison with the first two steps, and therefore, it could be treated as the rate-limiting step. Because the lines did not pass through the origin, intraparticle diffusion was not the only rate-limiting step [40] and boundary layer control may be involved in the process.

3.5. Effect of solution temperature and adsorption thermodynamics

3.5.1. Adsorption isotherms

Adsorption isotherms are widely used to describe the interaction between adsorbates and adsorbents. Parameters obtained from the adsorption isotherm models provide crucial information about the properties of the adsorbent as well as mechanisms of adsorption. Two important isotherms, the Langmuir, Freundlich isotherms, were considered in this study.

The Langmuir [41] isotherm assumes monolayer adsorption onto a surface containing a finite number of adsorption sites, and the adsorption is uniform with no transmigration of adsorbate in the surface plane [42]. The linear form of the Langmuir isotherm equation is represented as follows:

$$\frac{C_e}{Q_e} = \frac{1}{Q_m K_L} + \frac{1}{Q_m}C_e \tag{7}$$

where C_e is the equilibrium concentration of the adsorbate (mg/L), Q_e is the amount of adsorbate adsorbed per unit mass of adsorbent at equilibrium (mg/g), and Q_m is the theoretical maximum adsorption capacity (mg/g). The values of K_L and Q_m can be determined from the intercept and slope of the linear plot of C_e/Q_e vs. C_e.

In order to determine whether the adsorption process is favorable or unfavorable, a dimensionless constant separation factor or equilibrium parameter, R_L, is defined according to the following equation [42]:

$$R_L = \frac{1}{1 + K_L C_0} \tag{8}$$

where K_L is the Langmuir isotherm constant (L/g) and C_0 is the initial concentration of TMP (mg/L). The R_L value indicates if the isotherm is irreversible ($R_L = 0$), favorable ($0 < R_L < 1$), linear ($R_L = 1$), or unfavorable ($R_L > 1$).

The Freundlich isotherm is an empirical equation based on assuming that the adsorption process takes place on a heterogeneous surface through a multilayer adsorption mechanism and the adsorption capacity is related to the concentration of TMP at equilibrium [43]. The Freundlich equation is given by the following equation:

$$\ln Q_e = \ln K_F + \frac{1}{n}\ln C_e \tag{9}$$

where K_F and n are Freundlich constants, n gives an indication of how favorable the adsorption process is, while K_F ($mg\,g^{-1}\cdot(L/mg)^{1/n}$) relates to the adsorption capacity of the adsorbent. The values of K_F and $1/n$ were calculated from the intercept and slope of a plot of ln Q_e vs. lnC_e.

Sufficient information regarding the adsorption type was not provided by Langmuir and Freundlich isotherms. For clarifying the adsorption type, the data are applied to following the D–R isotherm equation [44]:

$$\ln Q_{eM} = \ln Q_{mM} - \beta\varepsilon^2 \tag{10}$$

where Q_{eM} is the amount sorbed onto the adsorbent (mmol/g), Q_{mM} represents maximum adsorption capacity of the sorbent (mmol/g), β is a constant related to sorption energy ($mol^2\,kJ^{-2}$), and ε is Polanyi sorption potential, the amount of energy required to pull a sorbed molecule from its sorption site to infinity which is equal to [44]:

$$\varepsilon = RT\ln\left(1+\frac{1}{C_e}\right) \tag{11}$$

where R is the gas constant ($\mathrm{kJ\,mol^{-1}k^{-1}}$); T is the temperature in Kelvin; and C_e is the equilibrium concentration in solution ($\mathrm{mol\,L^{-1}}$). Q_{mM} and β values can be determined from the intercept and the slope of the linear plot of experimental data of ln Q_{eM} vs. ε^2.

The sorption energy, E, calculated by using the expression is defined as below:

$$E = \frac{1}{(2\beta)^{0.5}} \tag{12}$$

If the sorption energy is the range of 8–16 kJ/mol, the adsorption type is designated for ion exchange mechanism. If sorption energy is smaller than 8 kJ/mol, the adsorption type is physical adsorption due to weak van der Waals forces [45].

The best-fit model was determined by the correlation coefficients together with the value of average percentage error (APE), as well as the sum of the absolute errors (EABS) which is defined as [46,47]:

$$\mathrm{APE}\ (\%) = \frac{\sum_{i=1}^{N}|Q_{\exp}-Q_{\mathrm{cal}}|/Q_{\exp}}{N}\times 100 \tag{13}$$

$$\mathrm{EABS} = \sum\nolimits_{i=1}^{N}|Q_{\exp}-Q_{\mathrm{cal}}| \tag{14}$$

where $Q_{\exp}$ and Q_{cal} (mg/g) are the experimental and calculated uptake amounts of TMP at equilibrium.

Sorption isotherms of TMP on feather-derived charcoal fit by the three isotherm models are displayed in Fig. 5, and the values of the constants calculated from the linear forms of the isotherms are summarized in Table 7. As shown in Fig. 5, the adsorption quantity decreased as the temperature increasing, indicating an exothermic process. At 293 and 303 K, Freundlich isotherm fits the data better than Langmuir isotherm. As the temperature rise to 313 K, Langmuir isotherm represented a better fit with the experimental data, which was also shown in Table 7. All the correlation coefficients (R^2) were higher than 0.96 at the three temperatures. The Langmuir isotherm model gave the highest R^2 values indicating that it appeared to be much more applicable than the Freundlich isotherm model. However, when APE and EABS values were considered, the adsorption was best described by the Freundlich models at the lower solution temperatures. Overall, the adsorption isotherms for the TMP-feather-derived charcoal system are explained better by the Freundlich isotherm at lower temperature while the Langmuir isotherm gave a better fit at higher temperature.

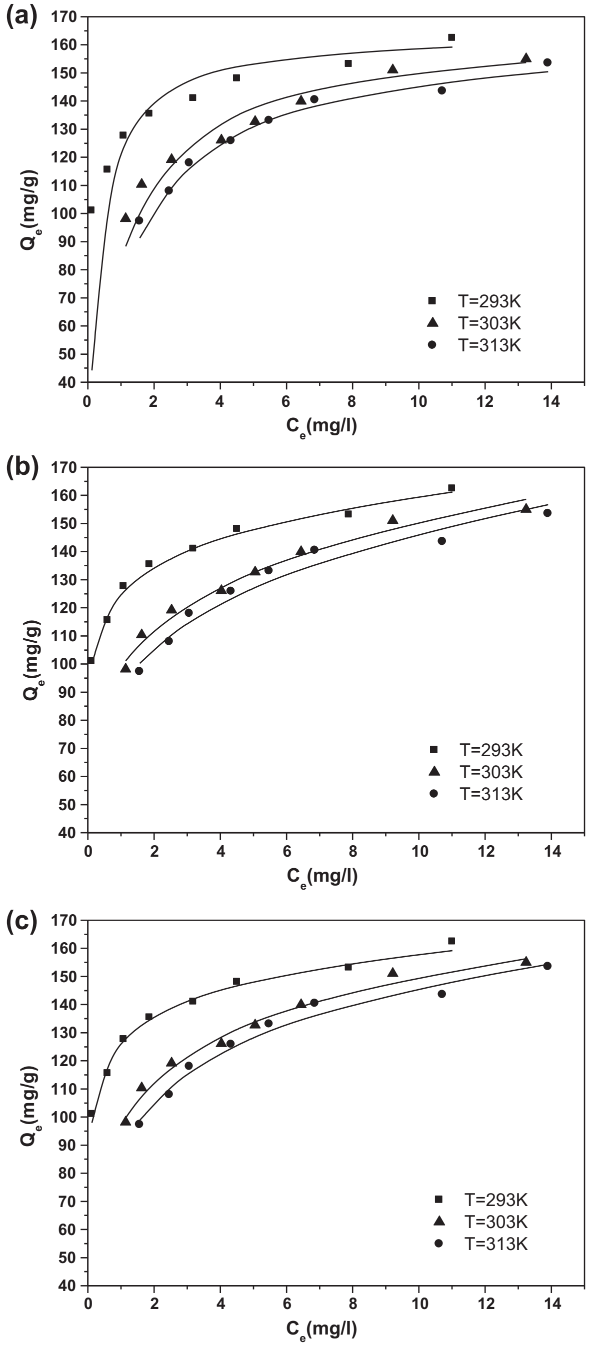

Fig. 5. Adsorption isotherms of TMP onto feather-derived charcoal described by the Langmuir model (a), Freundlich model (b) and the Dubinin–Radushkevich model (c). (agitation time = 60 h, sorbent dose = 0.2 g/L).

According to the parameters of D–R isotherm model, the value of E was in the range of 11.47–

Table 7
Langmuir, Freundlich, and Dubinin-Radushkevich isotherm model parameters and correlation coefficients

Isotherms	Parameters	293 K	303 K	313 K
Langmuir	Q_m/mg g^{-1}	164	164	164
	k_L/L g^{-1}	3,050	1,003	802
	R^2	0.9978	0.9978	0.9984
	APE	10.27	3.90	1.92
	EABS	91.92	36.51	18.46
Freundlich	k_F/mg g^{-1}(L/mg)$^{1/n}$	125	99	91
	n	9.50	5.45	4.89
	R^2	0.9913	0.9840	0.9650
	APE	1.19	1.63	2.63
	EABS	12.56	12.77	26.91
Dubinin–Radushkevich	β/mol^2/kJ^2	0.0016	0.0034	0.0037
	E/kJ/mol	17.68	12.13	11.62
	R^2	0.9714	0.9880	0.9840
	APE	1.91	1.31	1.63
	EABS	19.68	13.23	16.48

Table 8
Thermodynamic parameters for the adsorption of TMP onto feather-derived charcoal

T (K)	ΔG (kJ/mol)	ΔH (kJ/mol)	ΔS (J/mol K)
293	−36.37	−51.25	−51.91
303	−34.81		
313	−35.38		

17.68 kJ/mol, indicating ion change interaction was involved in the adsorption, but not the major mechanism. The adsorption of TMP onto feather-derived charcoal involves both physical and chemical adsorption. Low temperatures favor physical adsorption while a high temperature will benefit chemical adsorption, and physical adsorption is more obviously affected by temperature [48]. In short, the adsorption amount decreased at higher temperature. In addition, the values of R_L were in the range of 0.0074–0.0652 and the values of $1/n$ were less than 1, representing favorable adsorption.

3.5.2. Adsorption thermodynamics

The changes in standard free energy change (ΔG, kJ/mol), enthalpy change (ΔH, kJ/mol), and entropy change (ΔS, kJ/ (mol K)) were determined by the following equations [49]:

$$\Delta G = -RT \ln\,(1,000\,K_L) \tag{15}$$

$$\ln\,(1,000\,K_L) = \frac{\Delta S}{R} - \frac{\Delta H}{RT} \tag{16}$$

where R (8.314 J/[mol K]) is the universal gas constant, T (K) is the absolute temperature, and K_L (L/g) is Langmuir constant obtained from the plot of C_e/Q_e vs. C_e. The ΔH and ΔS values can be calculated from the slope and intercept of the plot of ln(1000 K_L) vs. $1/T$. The results were recorded in Table 8.

Negative ΔG values indicated the spontaneous nature of the adsorption process. The ΔG values were in the range of −34.81 to −36.37 kJ/mol and the ΔH value was −51.25 kJ/mol, indicating that the adsorptions are mainly physical in nature enhanced by chemisorptions [50]. The negative value of ΔH further confirmed that the adsorption processes were exothermic, which is consistent with the adsorption isotherms results.

4. Conclusion

In this work, chicken feathers were employed to prepare an activated charcoal adsorbent. The large amounts of oxygen-containing surface groups of feather-derived charcoal can explain the great adsorption capacity of TMP. Hydrophobic interaction was demonstrated to be the dominant adsorption mechanisms, while ion exchange and electrostatic interaction may also contribute to the adsorption. The combination could be explained by Lewis acid–base interaction, $-NH_2$ served as the Lewis base and the O-containing groups on carbon served as Lewis acids. The present work provides a new adsorbent material, which could advance the development of adsorption techniques for antibiotics removal from water.

Acknowledgements

This work was supported by the Natural Science Foundation for Distinguished Young Scholars of Shandong province (JQ201216), National Water Special Project (2012ZX07203-004) and Independent Innovation Foundation of Shandong University (2012JC029). The authors thank Dr. Pamela Holt for editing the manuscript prior to submission.

References

[1] V. McGovern, Recycling poultry feathers: More bang for the cluck, Environ. Health Perspect. 108 (2000) A366–A369.
[2] E. Vasileva-Tonkova, A. Gousterova, G. Neshev, Ecologically safe method for improved feather wastes biodegradation, Int. Biodeterior. Biodegr. 63 (2009) 1008–1012.
[3] S. Cheng, K. Lau, T. Liu, Y. Zhao, P.M. Lam, Y. Yin, Mechanical and thermal properties of chicken feather fiber/PLA green composites, Compos. Part B: Eng. 40 (2009) 650–654.
[4] A. Mittal, Adsorption kinetics of removal of a toxic dye, Malachite Green, from wastewater by using hen feathers, J. Hazard. Mater. 133 (2006) 196–202.
[5] A. Mittal, V. Thakur, V. Gajbe, Evaluation of adsorption characteristics of an anionic azo dye Brilliant Yellow onto hen feathers in aqueous solutions, Environ. Sci. Pollut. Res. 19 (2012) 2438–2447.
[6] A. Mittal, V. Thakur, V. Gajbe, Adsorptive removal of toxic azo dye Amido Black 10B by hen feather, Environ. Sci. Pollut. Res. 20 (2013) 260–269.
[7] F. Banat, S. Al-Asheh, D. Al-Rousan, Comparison between different keratin-composed biosorbents for the removal of heavy metal ions from aqueous solutions, Adsorpt. Sci. Technol. 20 (2002) 393–416.
[8] S. Al-Asheh, F. Banat, D. Al-Rousan, Adsorption of copper, zinc and nickel ions from single and binary metal ion mixtures on to chicken feathers, Adsorpt. Sci. Technol. 20 (2002) 849–864.
[9] G. de la Rosa, H.E. Reynel-Avila, A. Bonilla-Petriciolet, I. Cano-Rodriguez, C. Velasco-Santos, A.L. Martínez-Hernández, Recycling poultry feathers for Pb removal from wastewater: Kinetic and equilibrium studies, P. World Acad. Sci. Eng. Technol. 30 (2008) 1011–1019.
[10] S. Al-Asheh, F. Banat, D. Al-Rousan, Beneficial reuse of chicken feathers in removal of heavy metals from wastewater, J. Clean. Prod. 11 (2003) 321–326.
[11] X. Xue, X. He, Y. Zhao, Adsorptive properties of acid-heat activated rectorite for Rhodamine B removal: Equilibrium, kinetic studies, Desalin. Water Treat. 37 (2012) 259–267.
[12] L. Huang, Y. Sun, Q. Yue, Q. Yue, L. Li, B. Gao, Adsorption of Cd (II) on lotus stalks-derived activated carbon: Batch and column studies, Desalin. Water Treat. 41 (2012) 122–130.
[13] B.Z. Can, Z. Ceylan, M.M. Kocakerim, Adsorption of boron from aqueous solutions by activated carbon impregnated with salicylic acid: Equilibrium, kinetic and thermodynamic studies, Desalin. Water Treat. 40 (2012) 69–76.
[14] A. Mittal, Removal of the dye, Amaranth from waste water using hen feathers as potential adsorbent, Electron. J. Environ. Agric. Food Chem. 5 (2006) 1296–1305.
[15] V.K. Gupta, A. Mittal, D. Jhare, J. Mittal, Batch and bulk removal of hazardous colouring agent Rose Bengal by adsorption techniques using bottom ash as adsorbent, RSC Adv. 2 (2012) 8381–8389.
[16] H. Daraei, A. Mittal, M. Noorisepehr, F. Daraei, Kinetic and equilibrium studies of adsorptive removal of phenol onto eggshell waste, Environ. Sci. Pollut. R. (2012). 1–9 doi: 10.1007/s11356-012-1409-8
[17] A. Mittal, J. Mittal, L. Kurup, Utilization of hen feathers for the adsorption of indigo carmine from simulated effluents, J. Environ. Prot. Sci. 1 (2007) 92–100.
[18] A. Mittal, R. Jain, J. Mittal, S. Varshney, Removal of Yellow ME 7 GL from industrial effluent using electrochemical and adsorption techniques, Inter. J. Environ. Pollut. 43 (2010) 308–323.
[19] A.K. Sarmah, M.T. Meyer, A. Boxall, A global perspective on the use, sales, exposure pathways, occurrence, fate and effects of veterinary antibiotics (VAs) in the environment, Chemosphere 65 (2006) 725–759.
[20] S.A. Waksman, Microbial antagonisms and antibiotic substances, Soil Sci. 59 (1945) 482.
[21] S.D. Costanzo, J. Murby, J. Bates, Ecosystem response to antibiotics entering the aquatic environment, Mar. Pollut. Bull. 51 (2005) 218–223.
[22] J. Órfão, A. Silva, J. Pereira, S. Barata, I. Fonseca, P. Faria, M. Pereira, Adsorption of a reactive dye on chemically modified activated carbons—influence of pH, J. Colloid. Interface. Sci. 296 (2006) 480–489.
[23] H. Boehm, Some aspects of the surface chemistry of carbon blacks and other carbons, Carbon 32 (1994) 759–769.
[24] S. Gregg, K.S.W. Sing, Adsorption, Surface Area, and Porosity, 114 (1983) 279C.
[25] T. Budinova, E. Ekinci, F. Yardim, A. Grimm, E. Björnbom, V. Minkova, M. Goranova, Characterization and application of activated carbon produced by H_3PO_4 and water vapor activation, Fuel process. Technol. 87 (2006) 899–905.
[26] E. Fuente, J. Menendez, M. Diez, D. Suarez, M. Montes-Moran, Infrared spectroscopy of carbon materials: A quantum chemical study of model compounds, J. Phys. Chem. B 107 (2003) 6350–6359.
[27] A.N.A. El-Hendawy, Influence of HNO_3 oxidation on the structure and adsorptive properties of corncob-based activated carbon, Carbon 41 (2003) 713–722.
[28] J. Zawadzki, Infrared spectroscopy in surface chemistry of carbons, Chem. Phys. Carbon 21 (1989) 147–380.
[29] P. Vinke, M. Van der Eijk, M. Verbree, A. Voskamp, H. Van Bekkum, Modification of the surfaces of a gasactivated carbon and a chemically activated carbon with nitric acid, hypochlorite, and ammonia, Carbon 32 (1994) 675–686.
[30] G. Crini, H.N. Peindy, F. Gimbert, C. Robert, Removal of CI Basic Green 4 (Malachite Green) from aqueous solutions by adsorption using cyclodextrin-based adsorbent: Kinetic and equilibrium studies, Sep. Purif. Technol. 53 (2007) 97–110.
[31] Z. Bekçi, Y. Seki, M. Kadir Yurdakoç, A study of equilibrium and FTIR, SEM/EDS analysis of trimethoprim adsorption onto K10, J. Mol. Struct. 827 (2007) 67–74.
[32] Z. Bekçi, Y. Seki, M.K. Yurdakoç, Equilibrium studies for trimethoprim adsorption on montmorillonite KSF, J. Hazard. Mater. 133 (2006) 233–242.
[33] I.D. Mall, V.C. Srivastava, N.K. Agarwal, I.M. Mishra, Adsorptive removal of malachite green dye from aqueous solution by bagasse fly ash and activated carbon-kinetic study and equilibrium isotherm analyses, Colloids Surf. A 264 (2005) 17–28.

[34] Y. Önal, C. Akmil-Basar, Ç. Sarici-Özdemir, Investigation kinetics mechanisms of adsorption malachite green onto activated carbon, J. Hazard. Mater. 146 (2007) 194–203.

[35] G. Crini, Kinetic and equilibrium studies on the removal of cationic dyes from aqueous solution by adsorption onto a cyclodextrin polymer, Dyes Pigm. 77 (2008) 415–426.

[36] A. Altınışık, E. Gür, Y. Seki, A natural sorbent, *Luffa cylindrica* for the removal of a model basic dye, J. Hazard. Mater. 179 (2010) 658–664.

[37] O. Hamdaoui, E. Naffrechoux, Modeling of adsorption isotherms of phenol and chlorophenols onto granular activated carbon: Part I. Two-parameter models and equations allowing determination of thermodynamic parameters, J. Hazard. Mater. 147 (2007) 381–394.

[38] A. Singh, D. Singh, K. Panday, V. Singh, Wollastonite as adsorbent for removal of Fe (II) from water, J. Chem. Technol. Biotechnol. 42 (1988) 39–49.

[39] G. Boyd, A. Adamson, L. Myers, Jr, The exchange adsorption of ions from aqueous solutions by oganic zeolites. II. Kinetics1, J. Am. Chem. Soc. 69 (1947) 2836–2848.

[40] V. Poots, G. McKay, J. Healy, Removal of basic dye from effluent using wood as an adsorbent, Water Pollution Control Federation 50 (1978) 926–935.

[41] I. Langmuir, The adsorption of gases on plane surfaces of glass, mica and platinum, J. Am. Chem. Soc. 40 (1918) 1361–1403.

[42] T.W. Webi, R.K. Chakravort, Pore and solid diffusion models for fixed-bed adsorbers, AIChE J. 20 (1974) 228–238.

[43] M. Temkin, V. Pyzhev, Kinetics of ammonia synthesis on promoted iron catalysts, Acta Phys. chim. URSS 12 (1940) 327–356.

[44] A. Mittal, D. Jhare, J. Mittal, Adsorption of hazardous dye Eosin Yellow from aqueous solution onto waste material De-oiled Soya: Isotherm, kinetics and bulk removal, J. Mol. Liq. 179 (2012) 133–140.

[45] V. Sakthi, N.M. Andal, S. Rengaraj, M. Sillanpää, Removal of Pb (II) ions from aqueous solutions using Bombax ceiba saw dust activated carbon, Desalin. Water Treat. 16 (2010) 262–270.

[46] M. Dubinin, L. Radushkevich, Equation of the characteristic curve of activated charcoal, Chem. Zentralbl 1 (1947) 875.

[47] L. Wang, J. Zhang, R. Zhao, Adsorption of basic dyes on activated carbon prepared from Polygonum orientale Linn: Equilibrium, kinetic and thermodynamic studies, Desalination 254 (2010) 68–74.

[48] Y.C. Chiang, P.C. Chiang, C.P. Huang, Effects of pore structure and temperature on VOC adsorption on activated carbon, Carbon 39 (2001) 523–534.

[49] S.K. Milonjić, A consideration of the correct calculation of thermodynamic parameters of adsorption, J. Serb. Chem. Soc. 72 (2007) 1363–1367.

[50] R.I. Yousef, B. El-Eswed, A.a.H. Al-Muhtaseb, Adsorption characteristics of natural zeolites as solid adsorbents for phenol removal from aqueous solutions: Kinetics, mechanism, and thermodynamics studies, Chem. Eng. J. 171 (2011) 1143–1149.